Dry Metal Forming Open Access Journal

Fast Manuscript Track

Edited by Frank Vollertsen
Available online at elib.suub.uni-bremen.de

www.drymetalforming.de

Dry Met. Forming OAJ FMT 1 (2015) 152–158
Received 29 September 2015; published 04 November 2015

Tribological Behavior of $(Cr_{1-x}Al_x)N/WS_y$ PVD Tool Coatings for the Application in Dry Cold Forging of Steel

Kirsten Bobzin[1], Tobias Brögelmann[1], Nathan C. Kruppe[1], Serhan Bastürk*[1], Fritz Klocke[2], Patrick Mattfeld[2], Daniel Trauth[2]

[1]Surface Engineering Institute (IOT), RWTH Aachen University, Kackertstr. 15, 52072 Aachen, Germany
[2]Laboratory for Machine Tools and Production Engineering (WZL), RWTH Aachen University, Steinbachstr. 19, 52074 Aachen, Germany

Abstract

In cold forging processes, there is a strong demand to avoid lubricants due to economic, ecological and legislative aspects. PVD coatings on metal forming tools may enormously reduce tool and workpiece wear in cold forging or deliver special functions even in the absence of lubricants. However, the abdication of lubricants goes along with the requirement that the dry tribological system has to withstand the increased tribological loads. The extreme tribological conditions in cold forging process which can lead to contact pressures of more than p_{CP} = 2,500 MPa are critical for the success of a tool coating. $(Cr_{1-x}Al_x)N/WS_y$ coatings promise a solution to replace lubricants on highly forced tools in dry cold forging. Wear resistant $(Cr_{1-x}Al_x)N$ together with the self-lubricating WS_y deposited using PVD technology, offers an extension of tool life without lubricants. The aim of the current contribution is the evaluation of the tribological behavior of the $(Cr_{1-x}Al_x)N/WS_y$ PVD coatings under dry sliding conditions. At the Surface Engineering Institute (IOT) $(Cr_{1-x}Al_x)N/WS_y$ coatings with different chemical content ratios of WS_2 were deposited in an industrial high power pulsed magnetron sputtering (HPPMS) coating process. A special target which consists of a $Cr_{0.50}Al_{0.50}$ half and a WS_2 half in form of triangles was used, which led to a variation of the chemical composition of the deposited coatings according to the position of the sample on the holder. The coated samples of X155CrMoV12 (DIN 1.2379, AISI D2) tool material were investigated. A Pin-on-Disc (PoD) tribometer was used for tribological investigations of the coated samples under dry sliding conditions. Under the given tribological conditions depending on the WS_2 content, a significant wear reduction was observed for the $(Cr_{1-x}Al_x)N/WS_y$ coatings. A reduction of the friction coefficient from $\mu = 0.70$ for uncoated sample to $\mu = 0.25$ with the WS_y content was detected. The investigated $(Cr_{1-x}Al_x)N/WS_y$ coatings are a promising alternative to lubricants for the application in dry cold forging process of steel.

Keywords: Cold forging, HPPMS, (Cr,Al)N, WS_2, dry metal forming

1 Introduction

Cold forging is of great importance due to the maximum degree of material utilization and the associated energy and resource efficiency [1]. Cold forged parts are typically used within the drive technology, e.g. as driving shafts. In cold forging process, lubricants are applied between workpiece and forming tool in order to reduce friction. These lubricants containing harmful additives are questionable due to ecological, economic, and legislative reasons [2]. Therefore, there is a strong demand for using biodegradable lubricants without harmful additives. Tool coatings by means of physical vapor deposition (PVD) are an alternative to lubricants in cold forging processes for an environmentally friendly metal forming. Regarding to this demand, many studies were done within the Collaborative Research Center 442 (SFB 442) entitled 'Environmentally friendly tribological systems', which has been established by the German Research Foundation (DFG). A multilayer (Ti,Hf,Cr)N PVD coating for cold metal forming applications was developed using the arc ion plating technique by Lugscheider et al. [3]. This coating was enhanced using a CrN toplayer for the interaction with biodegradable lubricants for environmentally friendly metal forming [4]. As a next step, the avoidance of lubricant usage is the focus of many ongoing projects in metal forming which contributes significantly to waste

*E-mail address of corresponding author: basturk@iot.rwth-aachen.de

reduction in manufacturing processes and to the goal of a lubricant-free "green" factory. Nevertheless, none of the attempts to realize dry metal forming can meet the challenging demands of the dry cold forging process of steel so far [5].

High contact pressures of more than $\sigma_c = 2{,}500$ MPa are generated under extreme tribological conditions in the cold forging process [6]. The ternary PVD coating (Cr,Al)N is a promising candidate to withstand these extreme tribological loads. (Cr,Al)N coating is used for the application of cold forging due to its properties such as high hardness and good abrasion wear resistance [7, 8]. On the other hand, the coating has to reduce friction forces, which result in a reduced wear rate of the tools. Previous experimental investigations of (Cr,Al)N in both, lubricated contacts [9] and under dry running conditions [10] showed suitable properties for tribological applications. This (Cr,Al)N coating was enhanced by incorporation of vanadium (V) and tungsten (W) for friction reduction in tool applications for high temperatures between T = 600 °C and T = 800 °C by means of magnetron sputtering (MS) [11]. Another approach for the reduction of friction forces is the application of self-lubricating coatings. Transition metal dichalcogenide tungsten disulfide (WS_2) is a solid lubricant material, which is widely used in industry [12-14]. Its lubricating character is based on the anisotropic crystal layer structure which consists of tungsten (W) atom layers located between sulfur (S) atom-arrays. There is a strong covalent bonding between the atoms. However, the layers are loosely bound through comparably weak van der Waals forces. This structure results in the interlamellar mechanical weakness with low shear strength, resulting in a macroscopic lubricating effect [10, 14]. Application of WS_2 coatings on tools deposited by means of PVD reduces friction but only in vacuum or in inert gas environment [15]. Furthermore, another drawback of pure WS_2 is its mechanical properties. Pure WS_2 features a hardness which is lower than HU = 10 GPa [13]. The combination of the positive properties of hard coatings such as (Cr,Al)N and solid lubricant effect of WS_2 offers a solution for a "green" cold forging process. Coatings with a similar approach injecting nanoparticles of WS_2 during the reactive direct current magnetron sputtering (dcMS) of TiN coatings were prepared by Polcar et al. [16]. High power pulsed magnetron sputtering (HPPMS) technology represents an advancement of the dcMS technology. Using this technology, an extremely higher plasma density can be achieved in comparison to conventional dcMS due to high-energy pulses [17]. Coatings deposited by means of HPPMS show outstanding advantages with respect to good mechanical properties, dense morphology and an improved adhesion to the substrate [18]. Furthermore, another positive aspect of the HPPMS technology is the ability of coating of the complex-shaped tools with surfaces oriented non-parallel to the target, which is the case for the cold forging of steel [19].

The main focus of this study was set on the evaluation of the tribological behavior of HPPMS $(Cr_{1-x}Al_x)N/WS_y$ coatings. The structure of the paper is as follows. Firstly, experimental details of the deposition process of the HPPMS $(Cr_{1-x}Al_x)N/WS_y$ coatings and the analytical methods for the characterization of the coatings and compound properties as well as on the investigations by means of PoD tribometer are presented in Chapter 2. Afterwards, the results and discussion follow in Chapter 3. Concluding, the scientific findings are summarized and an outlook for future investigations is given in Chapter 4.

2 Experimental procedure

2.1 Deposition process of the $(Cr_{1-x}Al_x)N/WS_y$ coating

The investigated coatings in this study were deposited on substrates of X155CrMoV12 (DIN 1.2379, AISI D2; x_C=1.54, x_{Si}=0.35, x_{Mn}=0.31, x_P=0.028, x_S=0.008, x_{Cr}=11.52, x_{Mo}=0.73, x_V=0.94). All specimens (Ø = 20 mm, h = 8 mm) were hardened and tempered to a hardness of 60-62 HRC and polished to an arithmetic mean roughness of Ra = 0.02 µm. Prior to deposition, the specimens were cleaned in a multi-stage ultrasonic bath which contained alkaline solvents. Before the deposition, all specimens were cleaned in an in situ plasma treatment explained in [20]. An industrial coating unit CC800/9 Custom from CemeCon AG, Würselen, Germany was used. This unit is equipped with two conventional MS cathodes and two HPPMS cathodes. Figure 1 shows the schematic of the coating deposition setup.

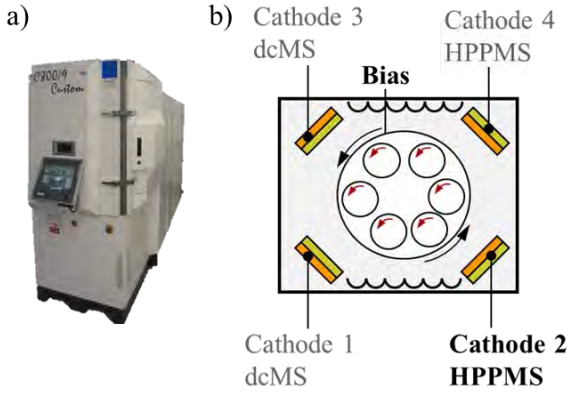

Figure 1: a) Industrial coating system and b) the schematic of the coating deposition setup (top view).

A special target (500 x 88 mm²) which consists of a $Cr_{0.50}Al_{0.50}$ half and a WS_2 half in form of triangles was used on HPPMS cathode no. 2 for the deposition. Schematic of the custom target and the sample positions is shown in Figure 2. This setup leads to a variation of chemical composition of the deposited coatings. The $Cr_{0.50}Al_{0.50}$ target section was produced by Plansee Composite Materials GmbH, Lechbruck am See, Germany, by means of sintering and has a purity of 99.9 %. The WS_2 target section has a purity of 99.5 %.

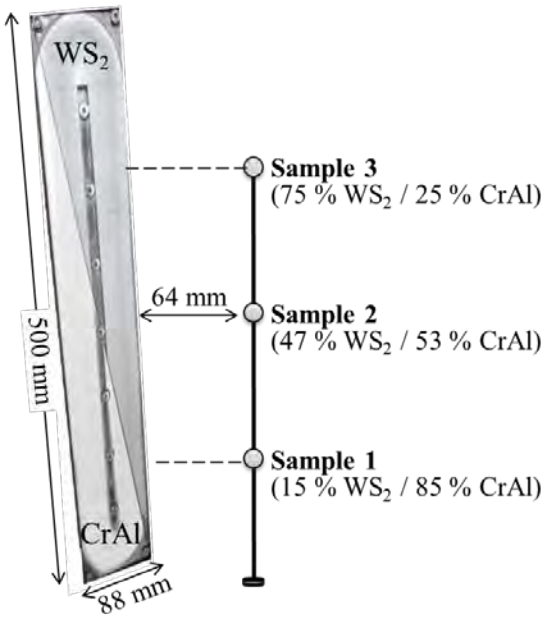

Figure 2: The custom target with sample configuration for the variation of chemical composition with ratios of line-of-sight target surfaces.

Synthesis strategy was based on the application of a gradient of the chemical composition of the coatings which was possible with such a special target. A total of three samples (sample 1, 2 and 3) was coated at different positions on the holder in order to achieve a variation of chemical composition due to the target configuration. The ratio of the (WS_2 surface/$Cr_{0.50}Al_{0.50}$ surface) increased with the increasing position of the sample on the holder. Considering this arrangement, WS_2 surface/$Cr_{0.50}Al_{0.50}$ surface ratios were varied between (15/85) and (75/25) as shown in Figure 2.

Table 1: Process parameters for the deposition of $(Cr_{1-x},Al_x)N/WS_y$ coatings.

Process parameter	Unit	Value
Time, t	min	350
Argon flux, Q(Ar)	sccm	200
Nitrogen flux, Q(N_2)	controlled over pressure	
Pressure, p	mPa	470
Substrate temperature, T	°C	305
Cathode mean power, P	W	2,500
Pulse frequency, f	Hz	500
Pulse length, t_{on}	µs	200
Bias voltage (dc), U_{Bias}	V	-120

A constant mean power of P = 2.5 kW was applied to the cathode in HPPMS mode. An HPPMS power supply GX 150/1000 (ADL GmbH, Darmstadt, Germany) was used. A pulse frequency of f = 500 Hz and a pulse length of t_{on} = 200 µs were chosen. Argon gas flow Q(Ar) was kept constant at Q(Ar) = 200 sccm. Nitrogen gas flow Q(N_2) was pressure controlled at p = 470 mPa. Conventional dc bias of U_{Bias} = -120 V was applied on substrate. Deposition temperature was kept at T = 305 °C in order to avoid annealing of temperature-sensitive substrate material. During the reactive sputtering, the samples were rotated in a twofold motion. Coatings were deposited for t = 350 min. The process parameters for deposition of $(Cr_{1-x},Al_x)N/WS_y$ coatings are listed in Table 1.

2.2 Analysis methods for the coating properties

The coating thickness and morphology were analyzed by using scanning electron microscopy (SEM) of type DSM 982 Gemini from Carl Zeiss GmbH, Jena, Germany. The chemical composition of the coatings was determined by using glow discharge optical emission spectroscopy (GDOES) in radio frequency (rf) mode. A GDOES profiler type JY 5000 RF from HORIBA Jobin Yvon Ltd., Kyoto, Japan was used. The crystallographic phase analysis of the coatings was carried out via X-ray diffractometry (XRD) using grazing incidence (GI) X-ray diffractometer XRD3003 from GE Energy Germany GmbH, Ratingen, Germany. Selected parameters were as follows: GI: $\omega = 3°$; diffraction angle 2θ: 15° to 90°; step width: s = 0.05°; step time: t = 5 s. All measurements were performed using Cu-Kα (wavelength $\lambda = 0.1540598$ nm) radiation operated at U = 40 kV and I = 40 mA. A NanoindenterTM XP from MTS Nano Instruments, Oak Ridge, Tennessee, USA with a Berkovich indenter was applied for the determination of the mechanical properties: universal hardness HU and the modulus of indentation E_{IT}. The penetration depth was kept below 10 % of the top layer thickness. Calculations of the modulus of indentation are based on Oliver and Pharr's equations [21]. A constant Poisson's ratio of $\upsilon = 0.25$ was assumed.

2.3 Investigation of the compound properties

Adhesion strength between the coating and substrate was quantitatively evaluated by scratch testing according to DIN EN 1071-3:2005 [22]. Scratch test conditions were identical in each case: applied loads F_S = 10-30 N, speed v_S = 0.5 mm/min, loading rate L = 10 N/min, and scratch length l = 4 mm. Scratch tracks were examined by means of confocal laserscanning microscopy (CLSM) with a VK-X210 microscope from Keyence GmbH, Neu-Isenburg, Germany. As a measure of the adhesion between coating and the substrate the critical loads (Lc_i) are determined at which the first signs of different coating failures are noted. Lc_1 is the load at which the undisturbed scratch shows first signs of failure in form of plastic deformation at scratch track's edge. At Lc_2 the coating starts to delaminate and the substrate material will be partly visible. At last, Lc_3 means the last at which the coating is completely torn apart from the substrate.

2.4 Investigations of tribological behavior

A PoD tribometer from CSM Instruments SA, Peseux, Switzerland was used for the investigation of the tribological behavior under dry sliding conditions. 16MnCr5 (DIN 1.7131, AISI 5115) pins (Ø = 6 mm,

Ra = 0.02 µm) were chosen as counterpart. 16MnCr5 is one of the typical tool materials in cold forging. The used pins were pressed in off center position onto the coated specimen with a constant load of F =10 N and a radius of r = 2.5 mm at room temperature T = 23 °C and controlled air atmosphere with a relative humidity of RH = 32 % (± 2). Relative velocity was v = 5 cm/s. Tribological investigation was carried out for a sliding distance of s = 200 m. Figure 3 shows the used PoD tribometer at IOT and the schematic of the PoD experiments. The wear tracks were examined using a confocal Raman spectrometer inVia REFLEX with a 532 nm laser from RENISHAW, Gloucestershire, United Kingdom.

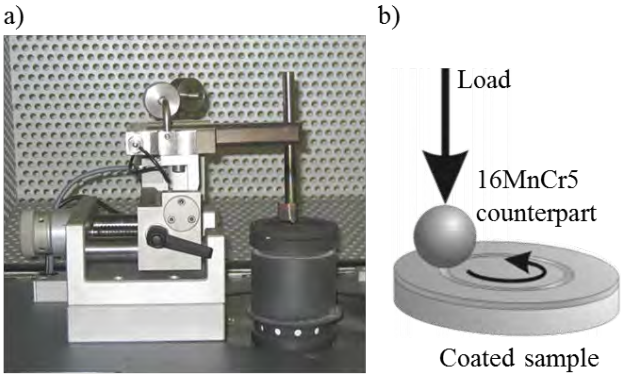

Figure 3: a) PoD tribometer at IOT and b) the schematic of the experiments.

3 Results and discussion

3.1 Coating properties

Cross section fractures of the three HPPMS $(Cr_{1-x}Al_x)N/WS_y$ coatings are shown in Figure 4. The thicknesses of the coatings are as follows: $d_{Sample1} = 3.85$ µm, $d_{Sample2} = 4.31$ µm and $d_{Sample3} = 4.58$ µm. With increasing position of the sample on the holder the coating thickness exhibits an increase (sample 1 to sample 3). Besides, a decrease of the Al- and Cr-contents of the coatings can be observed with increasing position of the sample in the holder in the experiment setup. Table 2 shows the chemical composition of the deposited coatings as measured by GDOES. Al content drops from $x_{Al} = 41.5$ at.% in sample 1 to $x_{Al} = 24.1$ at.% in sample 3. Decrease in the Cr-content is about $\Delta x_{Cr} = 7.5$ at.%. However, both the W and S contents almost quadruple with the increasing position of the sample in the holder from sample 1 to sample 3.

Table 2: Chemical composition of the $(Cr_{1-x}Al_x)N/WS_y$ coatings as determined by GDOES.

Element [at.%]	Sample 1	Sample 2	Sample 3
Al	41.5	34.6	24.1
Cr	31.7	30.0	24.2
N	17.3	15.0	15.0
S	3.3	7.0	12.5
W	6.3	13.4	24.3

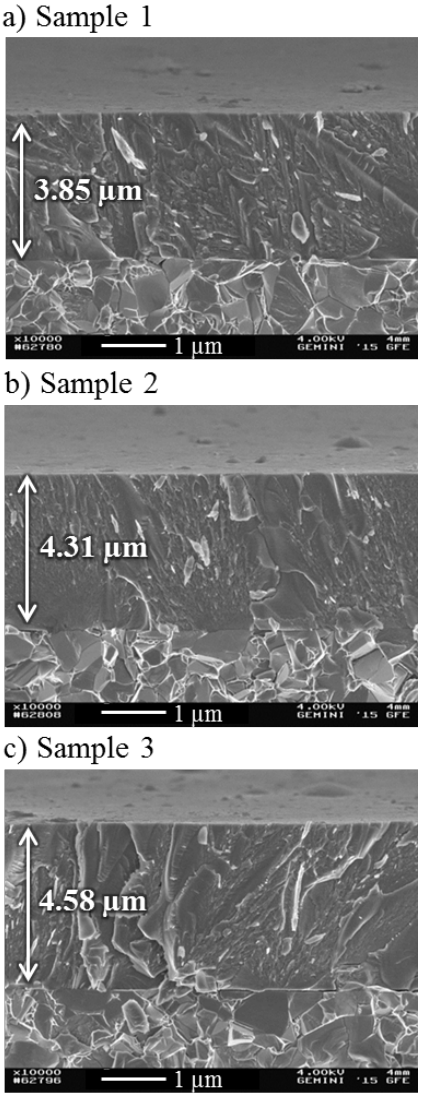

Figure 4: SEM cross section fractures of the $(Cr_{1-x}Al_x)N/WS_y$ coatings: a) Sample 1, b) Sample 2 and c) Sample 3.

Regarding the mechanical properties as universal hardness and the modulus of indentation, it must be stated that the HU^3/E_{IT}^2 ratio characterizes the resistance of the material to plastic deformation [23]. Therefore, a high HU and a low E_{IT} are aimed for tribological applications. Mechanical properties do not show extreme differences regarding the W- and S-contents. Sample 1 shows the highest mechanical properties which are as follows: HU = (16.4 ± 1.5) GPa and E_{IT} = (157.6 ± 22.8) GPa. HU^3/E_{IT}^2 ratio decreases with increasing W- and S-contents.

Table 3: Mechanical properties of the $(Cr_{1-x},Al_x)N/WS_y$ coatings as determined by nanoindentation.

	Sample 1	Sample 2	Sample 3
Universal hardness HU [GPa]	16.4 ± 1.5	14.8 ± 1.5	14.1 ± 1.1
Modulus of indentation E_{IT} [GPa]	157.6 ± 22.8	138.5 ± 22.5	144.97 ± 17.3
HU^3/E_{IT}^2	0.178	0.169	0.133

HPPMS $(Cr_{1-x}Al_x)N/MoS_y$ coatings were analyzed using XRD for the investigation of the phase composition. Figure 5 shows the XRD patterns of all deposited coatings. The increase of the substrate peaks, specially at $\omega = 37°$, can be due to the different coating thicknesses. All coatings present a crystal structure. Patterns indicate that the crystalline structure of the $(Cr_{1-x}Al_x)N$ phase is predominantly cubic. Neither hexagonal or tetragonal chromium nitride (CrN) phases nor the hexagonal aluminum nitride (AlN) phase are present in the coatings. Furthermore, no peaks of WS_y phase was detected for any $(Cr_{1-x}Al_x)N/MoS_y$ coating probably because of the amorphous structure.

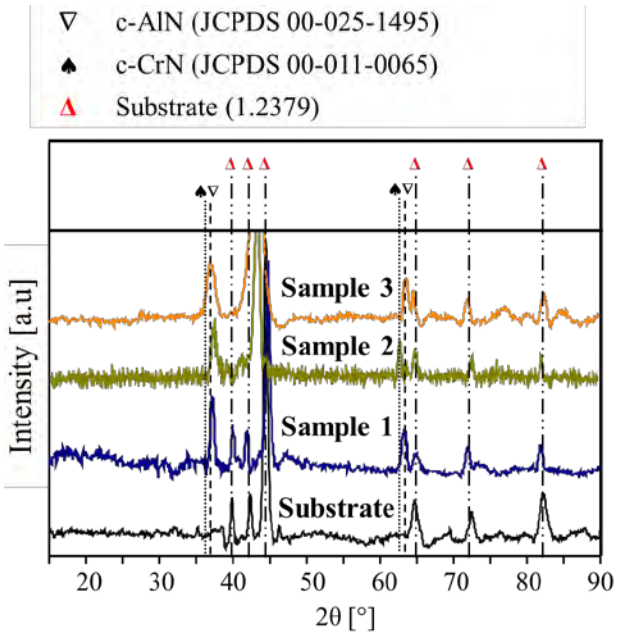

Figure 5: XRD patterns of the HPPMS $(Cr_{1-x}Al_x)N/WS_y$ coatings..

Scratch tests on all samples were done in order to evaluate the adhesion strength between the substrates and the HPPMS $(Cr_{1-x}Al_x)N/WS_y$ coatings. Figure 6 shows the investigation of scratch tracks test by means of CLSM. Critical loads at which the coating failures occur were determined. The arrow indicates the direction of the scratches. Critical load L_{C1}, where the first signs of the failure of the coating can be observed, decreases with the increasing W- and S-contents. Sample 1 has the first plastic deformation at scratch track's edge at $L_{C1} = 20$ N. For the samples 2 and 3, interfacial decohesion between the coating and substrate along the scratch track at L_{C2} and the completely delamination of the coating at L_{C3} appear at the same time as L_{C1} at $L_{C1,2,3} = 15$ N and 10 N respectively. It can be claimed that lower W- and S-contents are advantageous for better adhesion strength between coating and substrate. One solution to increase the obtained critical loads could be the application of a pure (Cr,Al)N bond coat between the substrate and $(Cr_{1-x}Al_x)N/WS_y$ coating. Previous studies have shown critical loads up to $L_{C3} = 60$ N of the same (Cr,Al)N coating without disulfides on the same substrate ALSI D2 [20]. Such a bond coat could improve the compound properties in the present work.

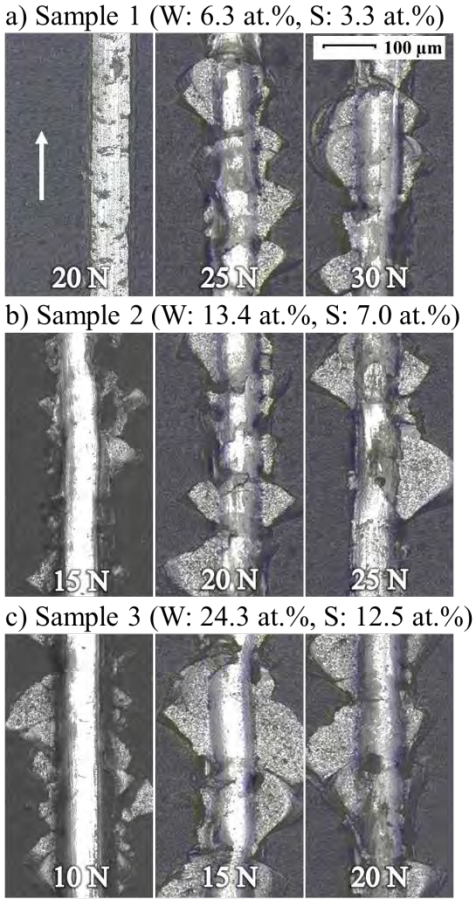

Figure 6: Scratch tracks at different loads of the $(Cr_{1-x}Al_x)N/WS_y$ coatings: a) sample 1, b) sample 2 and c) sample 3.

A PoD tribometer was used for the investigation of the friction behavior of the coated samples under dry sliding conditions. Investigations have shown that all three coated samples exhibit lower CoF compared to the uncoated substrate. The coating $(Cr_{31.7}Al_{41.5})N/WS_{0.52}$ (sample 3) shows the lowest CoF under the same conditions compared to the other coated samples which is $\mu = 0.25$. CoF of the sample 2 is $\mu = 0.3$, whereas sample 3 has a CoF of $\mu = 0.4$. Figure 7 shows the coefficient of friction CoF for the three coated samples as well as for the uncoated substrate as reference. The reason why sample 3 with the highest W- and S-contents shows the lowest CoF can be explained by the fact that sample 3 presents the highest HU^3/E_{IT}^2 ratio (compare Table 3) and therefore higher resistance to plastic deformation as well as to abrasion compared to the other coatings. For further investigation, the wear rate w and the wear volumes of the 16MnCr5 counterparts as well as of the HPPMS $(Cr_{1-x}Al_x)N/WS_y$ coated samples after tribological model tests by PoD tribometer were measured by means of CLSM. The results are shown in Table 4. Both, for the 16MnCr5 counterpart as well as for the samples, there is an increasing trend of the wear rates w and wear volumes with increasing W- and S-contents. Experiment of sample 1 indicates the lowest wear rate for the used counterpart $w = 4.1\ 10^3 \cdot \mu m^3/Nm$ and on the sample's surface $w = 0.9\ 10^3 \cdot \mu m^3/Nm$. There is not much difference between the wear rates for the counterparts while the difference between wear rates of the coated

samples is more than 10 times. The hypothesis with the HU^3/E_{IT}^2 ratio and the wear rates is supported by these results as well.

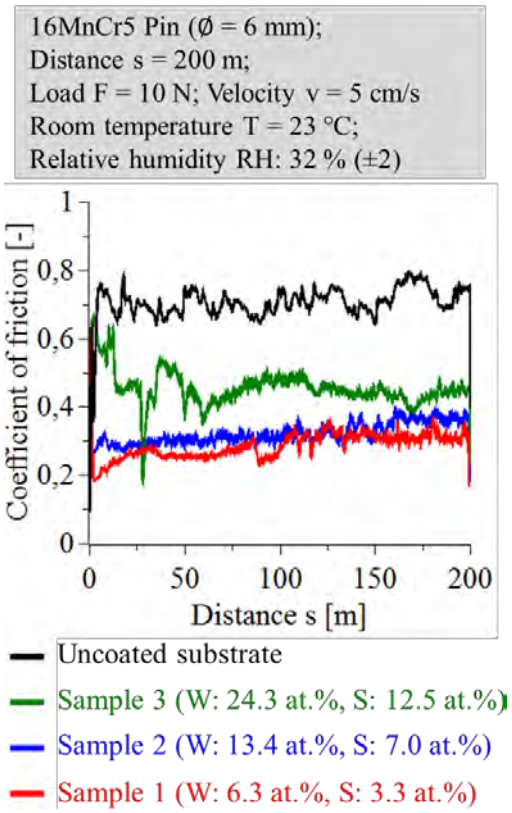

Figure 7: Coefficient of friction of the $(Cr_{1-x}Al_x)N/WS_y$ coated samples and uncoated substrate against 16MnCr5 using PoD tribometer.

Table 4: Measured wear rates and the wear volumes of the 16MnCr5 counterpart and the $(Cr_{1-x}Al_x)N/WS_y$ coatings after PoD experiments by means of CLSM.

	Sample 1	Sample 2	Sample 3
Wear rate w (counterpart) [$10^3 \cdot \mu m^3/Nm$]	4.1	8.4	25.2
Wear volume (counterpart) [$10^7 \cdot \mu m^3$]	0.8	1.7	5.0
Wear rate w (sample) [$10^3 \cdot \mu m^3/Nm$]	0.9	18.3	15.5
Wear volume (sample) [$10^7 \cdot \mu m^3$]	0.2	3.7	3.1

Measurements of the wear profile and tracks may confirm the assumed hypothesis. Figure 8 shows the wear profiles and tracks of the HPPMS $(Cr_{1-x}Al_x)N/WS_y$ coated samples. It can be observed that the profile depth becomes deeper and wider with the increasing W- and S-contents. Wear track on sample 1 shows a profile depth h = 1.5 µm which is lower than the coatings thickness of d = 3.85 µm. It can be concluded that the 16MnCr5 counterpart was in contact with the coating during the whole dry sliding model test. However, samples 2 and 3 show higher profile depths than their coating thicknesses. Therefore, it may be assumed that the coating was completely torn apart during the experiment and counterpart contacted substrate. Furthermore, the wear tracks on sample 1 and 2 were examined exemplary using Raman spectroscopy. Dots on the wear tracks in Figure 8 show the spots where the investigations were done. There is a clear shifting of the peaks. It can be assumed that the formation of self-lubricating sulphides is another aspect causing a reduction of the friction.

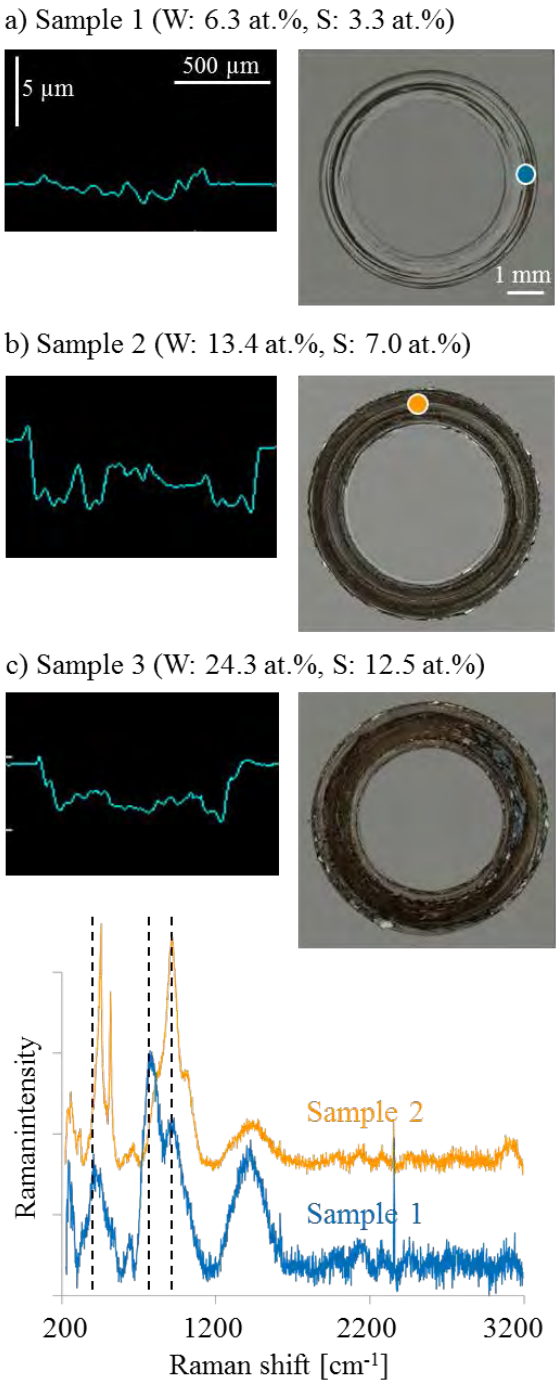

Figure 8: Wear profile and tracks of the HPPMS $(Cr_{1-x}Al_x)N/WS_y$ coated samples after PoD model tests by CLSM and exemplary Raman spectroscopy investigations of the wear tracks.

4 Conclusion and outlook

The absence of lubricants in metal forging significantly contributes to the aim of a lubricant-free "green" factory. However, the avoidance of lubricant usage goes along with the requirement that dry tribological system and the tool coatings have to withstand the increased tribological loads. In this contribution HPPMS $(Cr_{1-x}Al_x)N/WS_y$ coatings with different W- and S-contents were investigated regarding their tribological behavior. For this purpose, application oriented wear tests using a PoD tribometer were conducted. Wear tracks and volumes were investigated. HPPMS $(Cr_{31.7}Al_{41.5})N/WS_{0.52}$ coated sample (sample 3) shows the best results regarding tribological properties. Since the exemplary Raman spectroscopy results only give a first impression on the formation of self-lubricating sulphides, detailed investigations are needed. Furthermore, investigations with a novel Pin-on-Cylinder (PoC) tribometer [24] at Laboratory for Machine Tools and Production Engineering (WZL) will be performed to analyze the friction behavior which will constitute an important extension of this work. Based on the achieved results, $(Cr_{1-x}Al_x)N$ coatings in combination with self-lubricating WS_y deposited using HPPMS technology offers a great potential for lubricant-free "green" cold forging of steel.

Acknowledgements

The research was funded by the German Research Foundation (Deutsche Forschungsgemeinschaft DFG) within the priority program „Dry metal forming – sustainable production through dry processing in metal forming (Trockenumformen – Nachhaltige Produktion durch Trockenbearbeitung in der Umformtechnik (SPP 1676).

References

[1] F. Klocke: Manufacturing processes 4 - Forming, Springer, (2013).

[2] H. Czichos, K. Gerschwiler: Tribologie-Handbuch. Reibung und Verschleiß. Wiesbaden: Vieweg, (2007).

[3] E. Lugscheider, K. Bobzin, C. Pinero, F. Klocke, T. Massmann: Development of a superlattice (Ti,Hf,Cr)N coating for cold metal forming applications. Surface and Coatings Technology, 177-178 (2004) 616-622.

[4] K. Bobzin, N. Bagcivan, P. Immich, C. Warnke, F. Klocke, C. Zeppenfeld, P. Mattfeld: Advancement of a nanolaminated TiHfN/CrN PVD tool coating by a nano-structured CrN top layer in interaction with a biodegradable lubricant for green metal forming. Surface and Coatings Technology, 203 20-21 (2009) 3184-3188.

[5] F. Vollertsen, F. Schmidt: Dry Metal Forming: Definition, Chances and Challenges. Int. J. Precision Engineering and Manufacturing – Green Technology 1/1 (2014) 59–62.

[6] N. Bay, A. Azushima, P. Groche, I. Ishibashi, M. Merklein, M. Morishita, T. Nakamura, S. Schmid, M. Yoshida, Environmentally benign tribo-systems for metal forming, CIRP Annals - Manufacturing Technology 59 (2010) 760–780.

[7] J. Lin, B. Mishra, J.J. Moore, W.D. Sproul, Microstructure, mechanical and tribological properties of $Cr_{1-x}Al_xN$ films deposited by pulsed-closed field unbalanced magnetron sputtering (P-CFUBMS), Surface and Coatings Technology 201 (2006) 4329–4334.

[8] N. Bagcivan, K. Bobzin, R.H. Brugnara, Investigation of the properties of low temperature $(Cr_{1-x}Al_x)N$ coatings deposited via hybrid PVD DC-MSIP/HPPMS, Mat.-wiss. u. Werkstofftech. 44 (2013) 667–672.

[9] K. Bobzin, E. Lugscheider, M. Maes, P.W. Gold, J. Loos, M. Kuhn, High-performance chromium aluminium nitride PVD coatings on roller bearings, Surface and Coatings Technology 188-189 (2004) 649–654.

[10] K. Bobzin, E. Lugscheider, R. Nickel, N. Bagcivan, A. Krämer, Wear behavior of $Cr_{1-x}Al_xN$ PVD-coatings in dry running conditions, Wear 263 (2007) 1274–1280.

[11] K. Bobzin, N. Bagcivan, M. Ewering, R.H. Brugnara, S. Theiß: DC-MSIP/HPPMS (Cr,Al,V)N and (Cr,Al,W)N thin films for high-temperature friction reduction. Surface and Coatings Technology, 205 8–9 (2011) 2887-2892.

[12] T. Mang (Ed.), Lubricants and lubrication, Wiley-VCH, Weinheim (2007).

[13] C. Donnet, A. Erdemir, Solid Lubricant Coatings: Recent Developments and Future Trends Tribology Letters 17 (2004) 389–397.

[14] J.-F. Yang, B. Parakash, J. Hardell, Q.-F. Fang, Tribological properties of transition metal di-chalcogenide based lubricant coatings, Front. Mater. Sci. 6 (2012) 116–127.

[15] B. Deepthi, Harish C. Barshilia, K.S. Rajam, Manohar S. Konchady, Devdas M. Pai, Jagannathan Sankar, Alexander V. Kvit, Structure, morphology and chemical composition of sputter deposited nanostructured Cr–WS_2 solid lubricant coatings, Surface and Coatings Technology 205-2 (2010) 565-574.

[16] T. Polcar, D. Bharathi Mohan, C. Silviu Sandu, G. Radnoczi, A. Cavaleiro, Properties of nanocomposite film combining hard TiN matrix with embedded fullerene-like WS_2 nanoclusters, Thin Solid Films 519-10 (2011) 3191-3195.

[17] J. Alami, P.A.O. Persson, D. Music, J.T. Gudmundsson, J. Böhlmark, U. Helmersson, Ion-assisted physical vapor deposition for enhanced film properties on nonflat surfaces, Journal of Vacuum Science and Technology A: Vacuum, Surfaces and Films 23-2 (2005) 278.

[18] K. Bobzin, N. Bagcivan, P. Immich, S. Bolz, R. Cremer, T. Leyendecker, Mechanical properties and oxidation behaviour of (Al,Cr)N and (Al,Cr,Si)N coatings for cutting tools deposited by HPPMS, Thin Solid Films 517-3 (2008) 1251.

[19] N. Bagcivan, K. Bobzin, S. Theiß, $(Cr_{1-x}Al_x)N$: A comparison of direct current, middle frequency pulsed and high power pulsed magnetron sputtering for injection molding components, Thin Solid Films 528 (2013) 180-186.

[20] K. Bobzin, T. Brögelmann, S. Basturk, F. Klocke, P. Mattfeld, D. Trauth, Development of an in situ Plasma Treatment of X155CrMoV12 for a (Cr,Al)N PVD Tool Coating for Dry Metal Forming in Cold Forging, Dry Metal Forming Open Access Journal, 1 (2015) 57-62.

[21] W.C. Oliver, G.M. Pharr, An improved technique for determining hardness and elastic modulus using load and displacement sensing indentation experiments, Journal of Materials Research 7 (1992) 1564–1583.

[22] DIN EN 1071-3:2005 Advanced technical ceramics Methods of test for ceramic coatings Part 3: Determination of adhesion and other mechanical failure modes by a scratch test.

[23] J.Musil: Hard and superhard nanocomposite coatings. Surface and Coatings Technology, 125 (2000) 323-330.

[24] F. Klocke, D. Trauth, P. Mattfeld, A. Shirobokov, K. Bobzin, T. Brögelmann, S. Basturk, Multiscale FE-Studies of Contact Stresses of Dry and Lubricated Shot Peened Workpiece Surfaces, Dry Metal Forming Open Access Journal, 1 (2015) 11-16.